Pergamon

Int. J. Heat Mass Transfer. Vol. 38, No. 11, pp. 1945–1956, 1995
Copyright © 1995 Elsevier Science Ltd
Printed in Great Britain. All rights reserved
0017-9310/95 $9.50+0.00

0017-9310(94)00328-9

Mixed convection laminar flow and heat transfer of liquids in isothermal horizontal circular ducts

B. SHOME and M. K. JENSEN†

Department of Mechanical Engineering, Aeronautical Engineering and Mechanics, Rensselaer Polytechnic Institute, Troy, NY 12180-3590, U.S.A.

(*Received* 10 *June* 1994 *and in final form* 17 *October* 1994)

Abstract—Numerical analysis of thermally developing and simultaneously developing mixed convection flow and heat transfer with variable viscosity in an isothermal horizontal tube has been carried out. Parametric computations were performed to investigate the effect of inlet Prandtl number, inlet Rayleigh number, wall-to-inlet temperature difference, and inlet axial velocity profile on the Nusselt numbers and apparent friction factors for both heating and cooling conditions. The results indicate that the effect of variable viscosity is more pronounced on the friction factor than on Nusselt numbers. In addition, the effect of inlet Rayleigh number and inlet velocity profile on the Nusselt numbers and friction factors exists only in the near-inlet region. A parameter found by scaling analysis was used to empirically correlate the computed Nusselt number and the friction factor data and the available experimental Nusselt number data for both thermally developing and simultaneously developing flow and heat transfer. The developed correlations are more accurate, have wider ranges of applicability than those available in the literature, and should be of much use to designers.

INTRODUCTION

Mixed convection flow and heat transfer in smooth ducts has been studied extensively for a variety of duct geometries, duct orientations, and boundary conditions, as evident from refs. [1–3]. Mixed convection in horizontal ducts gives rise to secondary flows characterized by counter-rotating vortices and thermal stratification, which increases the pressure drop and heat transfer, reduces the thermal entrance length, and induces an early transition to turbulent flow. For ducts with a uniform heat flux (UHF) boundary condition (found in applications involving electrical heating or in fluid-to-fluid heat exchangers where the external heat transfer coefficient is low), a wall-to-bulk temperature difference exists throughout the length of the duct. As a result, secondary flow exists through out the duct length. In contrast, for ducts with a uniform wall temperature (UWT) boundary condition (e.g. condensers, evaporators, etc.), the secondary flow develops to a maximum intensity and eventually diminishes to zero as the wall-to-bulk temperature difference diminishes if the duct is long enough.

Experimental investigations have dealt with a variety of liquids (such as water, glycerol–water mixture, ethylene glycol, oil, etc.) but have been mostly limited to the thermally developing flow situation where a unheated flow length was provided to obtain a fully developed flow at the test section inlet. These investigations [4–14] have suggested a number of empirical correlations (see Table 1) for the length-averaged Nusselt number, where the effect of variable viscosity was taken into account through the use of the Sieder and Tate [15] type of correction. The effect of variable viscosity on free convection was neglected or was incorporated into the viscosity ratio correction term. Joshi and Bergles [16] pointed out that for ducts with isothermal walls, the exponent on the viscosity ratio correction factor in the Sieder and Tate correlation depends on the viscosity–temperature (ν–T) relationship of a particular fluid and changes significantly from the thermal entrance to the fully developed flow region. Due to these shortcomings, the available correlations are highly inaccurate and even the most accurate and widely recommended [1] correlation of Depew and August [11] has an uncomfortable error of $\pm 40\%$.

For simultaneously developing flow and heat transfer, the available experimental data and correlations are limited to air [7, 12]. In addition, no correlation for predicting the pressure drop is available. Since entrance length could be significant for large Prandtl number fluids ($Pr \geqslant 50$), a more extensive database and accurate correlations for predicting heat transfer and pressure drop are needed.

Numerous numerical investigations dealing with mixed convection flow and heat transfer in isothermal ducts exist. Hieber and Sreenivasan [17] carried out an approximate perturbation analysis for simultaneously developing flow and heat transfer. Their analysis was further extended by Yao [18] by including the interaction between the core and the near-wall boundary

† Author to whom correspondence should be addressed.

NOMENCLATURE

$a\ b\ c$	constants in viscosity-temperature model
A	tube cross-sectional area [m^2]
D	tube diameter [m]
f_{app}	apparent friction factor, $-\frac{1}{2}(d\bar{p}/dz)(D/\rho w_{in}^2)$
$\mathscr{F}$	$(1+\hat{v})/v^+$
g	gravitational constant, $= 9.81$ m s^{-2}
h	heat transfer coefficient [W m^{-2}K^{-1}]
Gr	Grashof number, $= g\beta\lvert\Delta T\rvert D^3/v^2$
Gz	Graetz number, $= \pi D\ Re\ Pr/4L$
k	thermal conductivity [W m^{-1} K^{-1}]
L	characteristic length [m]
Nu	Nusselt number, $= hD/k$
$\bar{p}\ \bar{P}$	average pressure [Pa]; average non-dimensional pressure $\bar{p}/\rho_{in}w_{in}^2$
p'	pressure driving cross-stream flow [Pa]
P'	non-dimensional pressure driving cross-stream flow $p'D^2/\rho_{in}\rho_{in}^2$
Pr	Prandtl number
$r\ R$	radial coordinate [m]; non-dimensional radial coordinate r/D
Ra	Rayleigh number, $= Gr\ Pr$
Re	Reynolds number, $= w_{in}D/v$
T	temperature [K]
$u\ v\ w$	azimuthal, radial, and axial velocity components, respectively [m s^{-1}]
$U\ V\ W$	non-dimensional velocities uD/v_{in}, vD/v_{in}, w/w_{in}, respectively
y	wall coordinate [m]
$z\ z^*\ z^+$	axial coordinate [m], $z/(DRe_{in})$, $z/(DRe_{in}Pr_{in})$.

Greek symbols

δ	hydrodynamic boundary layer thickness [m]
δ_t	thermal boundary layer thickness [m]
Δ	$\delta_{t,FC}/\delta_{t,NC} = Ra^{1/4}\mathscr{F}^{1/4}(z^+)^{1/2}$
ΔT	$(T_w - T_{in})$ [K]
γ	constant in viscosity–temperature model
ϕ	$(T-T_{in})/(T_w-T_{in})$
μ	dynamic viscosity [Pa s]
v	kinematic viscosity [m^2 s^{-1}]
v^+	v_b/v_w
$\hat{v}$	$(dv/dT)_b(T_w-T_b)/v_b$
ρ	fluid density[kg m^{-3}]
θ	angular coordinate [rad].

Subscripts

am	arithmetic mean
b	bulk
ch	characteristic
CP	constant property
f	film
FC	forced convection
in	inlet
lm	log mean
m	peripheral and length-averaged
NC	natural convection
TD	thermally developing
TR	transition
w	wall
0	reference.

layer flow. A more accurate finite difference solution was presented by Ou and Cheng [19]. However, to conserve computational time and preserve numerical stability, their solutions were carried out for low values of Rayleigh number ($Ra \leqslant 10^6$) using a large Prandtl number assumption ($Pr \to \infty$). Hishida *et al.* [20] relaxed the large Prandtl number assumption; however, the solutions were presented only for air. More recent studies include those by Pascal Courtier and Greif [21], Choudhury and Patankar [22], and Zhang and Bell [23], among others. However, none of these studies included variable viscosity in their analysis. The assumption of constant viscosity is unrealistic and could lead to large errors in predicting the heat transfer and pressure drop as the viscosity of most liquids vary significantly even at moderate wall-to-fluid temperature differences. Recently, Hwang and Lai [24] presented solutions for a wide range of Rayleigh numbers ($Ra = 0 \sim 10\times10^8$) using the assumptions of large Prandtl number, fully developed flow at the inlet, and constant viscosity. Correlations to predict the mean Nusselt numbers in the region where entrance and buoyancy effects balance each other were presented. However, due to the simplifying assumptions and the narrow range of validity, their correlation is of limited practical use.

For simultaneously developing flow, none of the the available numerical analyses has considered the effect of inlet geometry on mixed convection heat transfer and fluid flow. Since the inlet geometry influences the entrance velocity profile and, hence, the heat transfer and the onset of transitional flow, it is clear that inlet geometric effects should be included in the analysis for accurate and realistic predictions. However, it must be noted that it is difficult to quantify or model inlet geometry effects and experimental study may be the only recourse to investigate its influence. In this regard, some limited experimental results have been developed by Ghajar and Tam [25] for three different types of inlet geometries, namely: square-edged, bell-mouthed, and reentrant for UHF boundary condition. The effect of inlet geometry was reported to be negligible for laminar flow but had a considerable effect on transitional heat transfer.

An examination of the literature revealed that pressure drop correlations for developing laminar mixed

Table 1. Length-averaged Nusselt number correlations for developing laminar mixed convection flow and heat transfer in horizontal isothermal tubes

Reference	Correlation	Comments and limitations
Colburn [4]	$Nu_{am} = 1.75\left(\frac{\mu_b}{\mu_w}\right)^{1/3} Gz_b^{1/3}(1+CGr_f^{1/3})$ where $C = 0.015$	Air, water, oils $24 < L/d < 400$ $0.76 < Pr < 160$
Kern and Othmer [5]	$Nu_{am} = 10.45\left(\frac{\mu_b}{\mu_w}\right)^{0.14} Gz^{1/3}(1+0.01Gr^{1/3})/\ln Re$	Oil, $48 \leqslant L/D \leqslant 193$ $10^2 < Gr < 10^7$ $100 < Gz < 3000$ $39 < Pr < 2040$
Eubank and Proctor [6]	$Nu_{am} = 1.75\left(\frac{\mu_b}{\mu_w}\right)^{0.14}[Gz+C(Gr\,Pr\,D/L)^{0.4}]^{1/3}$ where $C = 12.6$	Oil, $61 < L/D < 235$ $10^5 < Ra < 10^8$ $12 < Gz < 4900$ $140 < Pr < 152\,000$
Jackson *et al.* [7]	$Nu_m = 2.67[Gz^2 + C(Gr_{lm}\,Pr)_w^{1.5}]^{1/6}$ where $C = 7.57\times10^{-5}$	Air, $L/D = 31$ $Gr \approx 10^6$ $33 < Gz < 3300$, $Pr = 0.7$
Oliver [8]	$Nu_{am} = 1.75\left(\frac{\mu_b}{\mu_w}\right)^{0.14}[Gz+C(Gr\,Pr\,L/D)^{0.7}]^{1/3}$ where $C = 5.6\times10^{-4}$	Glycerol–water, alcohol Water, $L/D = 72$ $29 < Gr < 1.6\times10^5$ $7 < Gz < 187$ $1.9 < Pr < 326$
Brown and Thomas [9]	$Nu_{am} = 1.75\left(\frac{\mu_b}{\mu_w}\right)^{0.14}[Gz+C(Gz\,Gr^{1/3})^{4/3}]^{1/3}$ where $C = 0.012$	Water, $36 < L/D < 108$ $10^4 < Gr < 10^6$ $19 < Gz < 112$ $3.5 < Pr < 6.8$
ESDU [10]	$Nu_{am} = 1.75\left(\frac{\mu_b}{\mu_w}\right)^{0.14}[Gz+CRa^{3/4}]^{1/3}$ where $C = 0.083$	—
Depew and August [11]	$Nu_{am} = 1.75\left(\frac{\mu_b}{\mu_w}\right)^{0.14}[Gz+C(Gz\,Gr^{1/3}Pr^{0.36})^{0.88}]^{1/3}$ where $C = 0.12$	Glycerol–water, alcohol Water, $L/D = 28.4$ $510 < Gr < 10^6$ $25 < Gz < 712$ $5.7 < Pr < 391$
Yousef and Tarasuk [12]	$Nu_{lm}\left(\frac{\mu_b}{\mu_w}\right)^{0.14} = 1.75[Gz+C(Gz^{1.5}Gr^{1/3})^{0.882}]^{1/3}$ where $C = 0.245$	Simultaneously developing, air $6 < L/D < 46$ $20 < Gz < 110$
Hieber [13]	$Nu_{am} = \left(\frac{\mu_b}{\mu_w}\right)^{0.14}[Nu_{FC}^3+Nu_{NC}^3]^{1/3}$ where $Nu_{NC} = [1.08\ln(1+1.14z^+Ra^{1/4})]/z^+$ and $Nu_{FC} = 1.62(z^+)^{-1/3}\exp(-16.4z^+) + 3.66[1-\exp(-27z^+)]$	$Ra \leqslant 4\times10^6$
Palen and Taborek [14]	$Nu_m = 2.5+4.55(Re^*D/L)^{0.37}Pr^{0.17}\left(\frac{\mu_b}{\mu_w}\right)^{0.14}$ where $Re^* = Re+0.8Gr^{0.5}\exp(-42/Gr^2)$	$0 < L/D < \infty$ $0 < Gr < 10^7$ $0.1 < Re < 2000$ $10^{-3} < \mu_b/\mu_w < 55$ $20 < Pr < 10^4$

convection flow are not available. The few available correlations [26, 27] were developed for fully developed flow and UHF boundary condition, and do not account for variable viscosity effects. For pure forced convection flow, the existing pressure drop correlations [3] are valid for fully developed flow and account for variable viscosity effect through the use of viscosity ratio correction factor. Such a type of correction has been shown to be inadequate in the developing region [16] for predicting heat transfer. Thus, the validity and accuracy of these correlations in the entrance region is questionable.

Thus, it is clear that although numerous studies (both experimental and numerical) have been undertaken to study mixed convection flow in isothermal ducts, little effort has been spent on analyzing variable viscosity effects, particularly for simultaneously developing flow and heat transfer. As a result, accurate correlations for predicting heat transfer and pressure drop are lacking. Therefore, the present investigation was initiated, (i) to perform scaling analysis and find parameter(s) which would correlate the present and the existing data better, (ii) to numerically simulate mixed convection flow and heat transfer in a horizontal isothermal smooth tube by including variable viscosity effects, and (iii) to accurately correlate the average Nusselt number and apparent friction factor for such flows. The analysis presented here will be limited to the UWT boundary condition because it closely simulates heat exchangers with fluid-to-fluid heating or cooling. In addition, due to lack of information, an uniform inlet velocity profile will be assumed for the simultaneously developing flow situation. Furthermore, unless otherwise stated, all the properties used in this analysis will be evaluated at the average bulk temperature to maintain consistency with the experimental results.

SCALING ANALYSIS

In order to perform the scaling analysis, the boundary layer equations for conservation of mass, momentum, and energy for pure forced convection flow in a circular duct are considered. These equations in a confined axisymmetric flow coordinate system [28] are:

$$\frac{\partial}{\partial y}(rv)+\frac{\partial}{\partial z}(rw) = 0 \tag{1}$$

$$v\frac{\partial w}{\partial y}+w\frac{\partial w}{\partial z} = -\frac{1}{\rho}\frac{\mathrm{d}p}{\mathrm{d}z}+\frac{1}{r}\frac{\partial}{\partial y}\left(r\nu\frac{\partial w}{\partial y}\right) \tag{2}$$

$$v\frac{\partial T}{\partial y}+w\frac{\partial T}{\partial z} = \frac{\alpha}{r}\frac{\partial}{\partial y}\left(r\frac{\partial T}{\partial y}\right). \tag{3}$$

In the boundary layer regime, the changes in y, z, w, and T are scaled by $y \sim \delta$, $z \sim L$, $w \sim w_{\mathrm{in}}$, and $T \sim (T_{\mathrm{w}}-T_{\mathrm{b}})$. Thus, from the continuity equation, the scale for the radial velocity is $v \sim w_{\mathrm{in}}\,\delta/L$. The scale for the inertia terms is then w_{in}^2/L. The scale for the friction term can be derived by assuming $\nu = \nu(T)$ and expanding the friction term using chain rule as:

$$\frac{1}{r}\frac{\partial}{\partial y}\left(r\nu\frac{\partial w}{\partial y}\right) = \nu\frac{\partial^2 w}{\partial y^2}+\frac{\mathrm{d}\nu}{\mathrm{d}T}\frac{\partial T}{\partial y}\frac{\partial w}{\partial y}. \tag{4}$$

The scale for the friction term can then be obtained by rearrangement of the above equation by substituting the scales of each individual terms as friction $\sim w_{\mathrm{in}}\nu(1+\hat{\nu})/\delta^2$. The scale for the pressure gradient term can be obtained by applying Bernoulli equation in the core region since by definition the core flow is inviscid as:

$$\frac{1}{\rho}\frac{\mathrm{d}P}{\mathrm{d}z} = w\frac{\partial w}{\partial z} \sim w_{\mathrm{in}}^2/L. \tag{5}$$

Finally, invoking a balance between inertia, pressure, and frictional force and introducing the Reynolds number, we obtain

$$\delta/D \sim \left(\frac{\mathscr{F}L}{DRe_{\mathrm{in}}}\right)^{1/2}. \tag{6}$$

Incorporating the result $\delta/\delta_{\mathrm{t}} \sim Pr^{-1/2}$ from boundary layer theory [29], we obtain

$$(\delta_{\mathrm{t}}/D)_{\mathrm{FC}} \sim \left(\frac{\mathscr{F}L}{DRe_{\mathrm{in}}Pr_{\mathrm{in}}}\right)^{1/2}. \tag{7}$$

Since the length L is arbitrary, we can replace L by z and rewrite equation (7) as:

$$(\delta_{\mathrm{t}}/D)_{\mathrm{FC}} \sim (\mathscr{F}z^+)^{1/2}. \tag{8}$$

To account for the variable viscosity effect, the term $\mathscr{F}$, where $\mathscr{F} = (1+\hat{\nu})/\nu^+$, includes both the viscosity ratio, ν^+, and the non-dimensional slope of the $\nu-T$ curve, $\hat{\nu}$. For constant viscosity, $\mathscr{F} = 1$ and $Nu_{\mathrm{FC}} \sim (D/\delta_{\mathrm{t}})_{\mathrm{FC}} \sim (z^+)^{-1/2}$ which agrees with the result given in ref. [29].

For pure natural convection flow, following ref. [29], the momentum equation for $Pr \gg 1$ (applicable to many liquids) is a statement of balance between frictional and buoyancy forces, the scales of which are $\nu v_{\mathrm{ch}}(1+\hat{\nu})/\delta_{\mathrm{t}}^2$ and $g\beta(T_{\mathrm{w}}-T_{\mathrm{b}})$, respectively. The scale for the characteristic velocity, v_{ch}, that scales the secondary flow brought upon by buoyancy effects is given in ref. [29] as $v_{\mathrm{ch}} \sim \alpha D/\delta_{\mathrm{t}}^2$. Replacing v_{ch} in the frictional and buoyancy scales and equating these, we obtain:

$$(\delta_{\mathrm{t}}/D)_{\mathrm{NC}} \sim (Ra/\mathscr{F})^{-1/4}. \tag{9}$$

For constant viscosity ($\mathscr{F} = 1$), we have $Nu_{\mathrm{NC}} \sim (D/\delta_{\mathrm{t}})_{\mathrm{NC}} \sim Ra^{1/4}$, a result which agrees with that in ref. [29].

Next, we define a parameter, Δ, given by

$$\Delta = \frac{(\delta_{\mathrm{t}}/D)_{\mathrm{FC}}}{(\delta_{\mathrm{t}}/D)_{\mathrm{NC}}} = Ra^{1/4}\mathscr{F}^{1/4}(z^+)^{1/2} \tag{10}$$

which is a measure of the relative strengths of the two different modes (forced and natural convection) of heat transfer. Since the type of convection mechanism is decided by the smaller of the two scales, $\delta_{\mathrm{t,FC}}$ or $\delta_{\mathrm{t,NC}}$, the transition from forced to natural convection occurs approximately at $\Delta = 1$. When $\Delta < 1$, forced convection dominates and when $\Delta > 1$, natural convection dominates. Furthermore, because the parameter Δ suitably combines the parameters governing variable viscosity effects ($\mathscr{F}$), natural convection effects (Ra), and forced convection effects (z^+), it could be used for correlating Nusselt numbers and friction factors for mixed convection flow and heat transfer with variable viscosity.

NUMERICAL ANALYSIS

The problem investigated is a three-dimensional parabolic, internal flow problem. In the present analysis, a parabolized Navier–Stokes formulation is followed which allows the pressure, p, to be divided into two parts as

$$p(r,\theta,z) = \bar{p}(z)+p'(r,\theta). \tag{11}$$

The non-dimensional equations of mass, momentum, and energy conservation in r–θ–z polar coordinates with the assumptions of (i) steady, laminar flow, (ii) negligible viscous dissipation, axial conduction in fluid and duct wall, (iii) applicability of the Boussinesq approximation, and (iv) variable viscosity are:

$$\frac{1}{R}\frac{\partial U}{\partial\theta}+\frac{1}{R}\frac{\partial}{\partial R}(RV)+\frac{\partial W}{\partial z^*}=0 \tag{12}$$

$$\frac{1}{R}\frac{\partial}{\partial\theta}(UU)+\frac{1}{R}\frac{\partial}{\partial R}(RVU)+\frac{\partial}{\partial z^*}(WU)+\frac{UV}{R}=-\frac{1}{R}\frac{\partial P'}{\partial\theta}+\frac{1}{R^2}\frac{\partial}{\partial\theta}\left(\frac{\nu}{\nu_{in}}\frac{\partial U}{\partial\theta}\right)+\frac{\partial}{\partial R}\left[\frac{\nu}{\nu_{in}R}\frac{\partial(RU)}{\partial R}\right]+\frac{2\nu}{\nu_{in}}\frac{1}{R^2}\frac{\partial V}{\partial\theta}-Gr_{in}\phi\sin\theta \tag{13}$$

$$\frac{1}{R}\frac{\partial}{\partial\theta}(UV)+\frac{1}{R}\frac{\partial}{\partial R}(RVV)+\frac{\partial}{\partial z^*}(WV)-\frac{U^2}{R}=-\frac{\partial P'}{\partial R}+\frac{1}{R^2}\frac{\partial}{\partial\theta}\left(\frac{\nu}{\nu_{in}}\frac{\partial V}{\partial\theta}\right)+\frac{\partial}{\partial R}\left[\frac{\nu}{\nu_{in}R}\frac{\partial(RV)}{\partial R}\right]-\frac{2\nu}{\nu_{in}R^2}\frac{\partial U}{\partial\theta}+Gr_{in}\phi\cos\theta \tag{14}$$

$$\frac{1}{R}\frac{\partial}{\partial\theta}(UW)+\frac{1}{R}\frac{\partial}{\partial R}(RVW)+\frac{\partial}{\partial z^*}(WW)=-\frac{d\bar{P}}{dz^*}+\frac{1}{R^2}\frac{\partial}{\partial\theta}\left(\frac{\nu}{\nu_{in}}\frac{\partial W}{\partial\theta}\right)+\frac{1}{R}\frac{\partial}{\partial R}\left(\frac{\nu R}{\nu_{in}}\frac{\partial W}{\partial R}\right) \tag{15}$$

$$\frac{1}{R}\frac{\partial}{\partial\theta}(U\phi)+\frac{1}{R}\frac{\partial}{\partial R}(RV\phi)+\frac{\partial}{\partial z^*}(W\phi)=\frac{1}{Pr_{in}}\left\{\frac{1}{R^2}\frac{\partial^2\phi}{\partial\theta^2}+\frac{1}{R}\frac{\partial}{\partial R}\left(R\frac{\partial\phi}{\partial R}\right)\right\}. \tag{16}$$

Equations (12)–(16) were solved along with inlet and boundary conditions of

$$U=V=W=0 \quad \text{and} \quad \phi=1 \quad \text{at} \quad R=0.5$$

$$U=\frac{\partial V}{\partial\theta}=\frac{\partial W}{\partial\theta}=\frac{\partial\phi}{\partial\theta}=0 \quad \text{at} \quad \theta=0 \quad \text{and} \quad \pi$$

$$U=V=\phi=0 \quad \text{and}$$

$$W=\begin{cases}2-8R^2 & \text{thermally developing}\\ 1 & \text{simultaneously developing}\end{cases} \quad \text{at} \quad z^*=0 \tag{17}$$

by using the general purpose finite-volume commercial program PHOENICS which is based on the SIMPLEST algorithm [30]. A non-uniform grid was used for the radial and axial directions to concentrate more grid points near the wall and the inlet, respectively, while a uniform grid was used for the azimuthal direction. The radial power-law grid was generated by $R_j = 0.5-0.5[(N-j)/N]^{1.5}$, where N is the total number of radial grid points, and the axial grid was generated by varying the distance between two consecutive grid points as $\Delta z^*_{k+1} = 1.1\Delta z^*_k$.

The apparent friction factor, which is based on total pressure drop, takes into account both frictional pressure drop and the change in momentum rate (due to change in velocity profile) in the hydrodynamic entrance region. Following ref. [31], the apparent friction factor was calculated as:

$$f_{app}Re_{in}=\frac{4}{\pi z^*}\int_0^{z^*}\int_0^{\pi}\nu^+(\partial W/\partial R)_w\,d\theta\,dz^*+\frac{1}{2Az^*}\int_A(W^2-W_{in}^2)\,dA. \tag{18}$$

From the computed non-dimensional velocity and temperature fields, the average Nusselt numbers were calculated as:

$$Nu_m=\frac{2}{\pi z^+}\int_0^{z^+}\int_0^{\pi}\frac{(\partial\phi/\partial R)_w}{(1-\phi_b)}\,d\theta\,dz^+$$

$$Nu_{am}=\frac{1}{4z^+}\frac{\phi_b}{1-\phi_b/2}$$

$$\text{where} \quad \phi_b=\left(\int_A W\phi\,dA\right)\Big/\left(\int_A W\,dA\right). \tag{19}$$

VISCOSITY MODEL

As seen from the scaling analysis, the parameters $\hat{\nu}$ and ν^+ describe the variable viscosity effects. Since these parameters depend on the ν–T behavior, it is imperative that an accurate ν–T model be used to ensure accurate prediction of Nusselt numbers and friction factors. An examination of the literature revealed that four different ν–T models for liquids have been used most often. These models along with representative refs. [16, 32–34] are shown in Table 2. To assess their accuracy for a wide range of Pr ($2 \leqslant Pr \leqslant 1250$), these models were fitted to the ν–T data for water, ethylene glycol, and a heat transfer oil. Model 4 consistently provided the best fit as compared to the other three models. This is not surprising since model 4 has the largest number of adjustable constants. Thus, it was concluded that model 4 is the best representation of the ν–T variation for most liquids. In this investigation, model 4 was used to represent the ν–T variation of water, ethylene glycol, and a heat transfer oil, PARATHERM-NF. To ensure an accurate fit, separate regression analyses were carried out for each of the ΔT ranges studied. The values of the ν–T model constants for different fluids and for different ranges studied are shown in Table 3.

RESULTS AND DISCUSSION

To establish grid independence for z^+ as small as 10^{-6}, numerical experiments were carried out for

Table 2. Viscosity temperature models of liquids

Model	ν–T relation	Representative reference
1	$\nu/\nu_0 = \exp[-\gamma(T-T_0)]$	Joshi and Bergles [16]
2	$\nu/\nu_0 = 1/(1+\gamma\phi)$	Yang [32]
3	$\nu/\nu_0 = \exp[\gamma(1/T-1/T_0)]$	Rosenberg and Hellums [33]
4	$\ln\ln(\nu/10^{-6}-c) = a\ln T+b$	Test [34]

Table 3. Constants used in the viscosity-temperature model

Fluid	T_{in} (K)	ΔT (K)	a	b	c
Water	283	30	−5.8950	33.0316	−0.88
Water	360	−30	−5.8950	33.0316	−0.88
Ethylene–glycol	300	20	−4.3200	26.6345	−0.80
Ethylene–glycol	300	−20	−4.3113	25.5855	−0.80
PARATHERM-NF	283	30	−4.7294	28.2715	0.50
PARATHERM-NF	313	30	−4.1640	25.0254	0.50
PARATHERM-NF	313	−30	−4.7294	28.2715	0.50
PARATHERM-NF	368	10	−5.2636	31.4674	0.50
PARATHERM-NF	368	−10	−4.7669	28.5382	0.50
PARATHERM-NF	368	30	−5.3586	31.1902	0.50
PARATHERM-NF	368	−30	−4.6920	28.0935	0.50

$Pr_{in} = 1250$, $Ra_{in} = 10^5$, and $\Delta T = 30$ K using $60\times30\times154$ and $60\times60\times154$ ($r\times\theta\times z$) grids. The computed average Nusselt number and apparent friction factors for these two grids differed by less than 1% for both thermally and simultaneously developing flow and heat transfer. Hence, to conserve computational time a $60\times30\times154$ grid was used in this study. The initial Δz^* was chosen as 10^{-8} to obtain accurate results in the near-inlet region; smaller values were avoided for computational economy.

Parametric computations were conducted for both thermally and simultaneously developing flow and heat transfer for $Pr_{in} = 2$, 10, 50, 150, 200, and 1250; $Ra_{in} = 10^5$, 10^6, 10^7, 10^8; $\Delta T = -30$, -20, -10, 10, 20, 30 K; and for constant viscosity. The numerical scheme was validated by comparing the pure forced convection ($Ra_{in} = 0$) constant property results against the classical Graetz solution [31]. Close agreement (in the range 0.1–0.6%) was obtained. As a further check, the results for thermally developing mixed convection flow ($Ra_{in} = 8\times10^5$, $Pr_{in} = 10^3$, constant viscosity) were compared against the numerical solution of Ou and Cheng [19]. The agreement in Nu_{am} was within 3.5%. Furthermore, computed Nu_{am} were compared against the experimental data tabulated by Oliver [8] for 80–20 glycerol–water solution and by Depew and August [11] for water with two different cooling conditions. The ν–T variation of these fluids was incorporated in the analysis by fitting model 4 to the property data. The agreement is satisfactory as shown in Fig. 1, considering the experimental uncertainty (generally in the range 10–15% for Nusselt numbers). It may be noted that the agreement between the experimentally determined and the present numerically calculated Nu_{am} is slightly better than that obtained in ref. [19]. This is probably due to inclusion of variable viscosity and relaxation of the infinite Prandtl number assumption in the present analysis. In addition, the streamline patterns (indicating two counter-rotating vortices) at various axial locations for the range of parameters investigated were qualitatively similar to those present in the literature [19, 24]. The streamlines and isotherms for the variable and constant viscosity were qualitatively similar to each other. These plots are not shown in this paper to preserve space.

The average Nusselt number, Nu_m, for thermally developing mixed convection flow for different ranges of Pr_{in}, Ra_{in}, and ΔT is shown in Fig. 2. From Figs. 1 and 2 it is clear that in the near inlet region forced

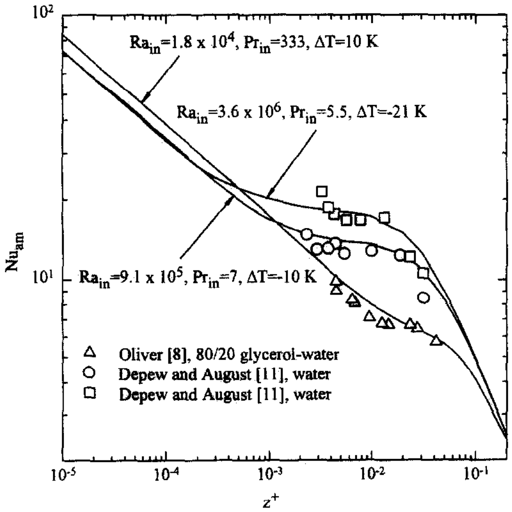

Fig. 1. Comparison of numerically evaluated average Nusselt number for thermally developing flow and heat transfer with available experimental results.

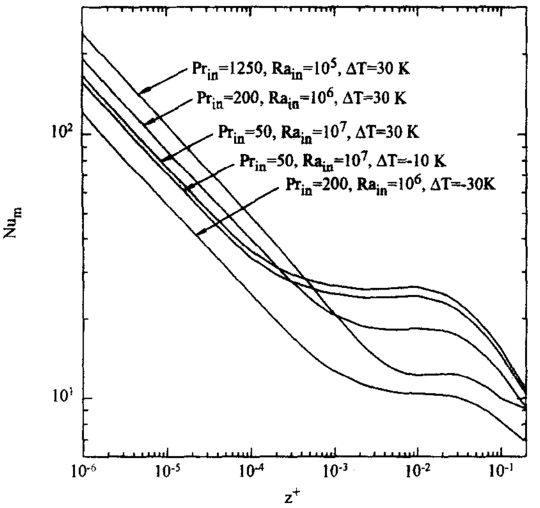

Fig. 2. Average Nusselt numbers for thermally developing mixed convection flow and heat transfer.

convection dominates, and the Nusselt numbers are influenced by the entrance and variable viscosity effects only.

For simultaneously developing mixed convection flow and heat transfer, the parameters Pr_{in}, Ra_{in}, and ΔT were varied to investigate their effect on the average Nusselt number and the apparent friction factor. The effect of Pr_{in} on Nu_m and $f_{app}Re_{in}$ for $\Delta T = 30$ K and $Ra_{in} = 10^6$ are shown in Fig. 3(a) and (b), respectively. In the near-inlet region ($z^+ \leqslant 2 \times 10^{-5}$), the Nu_m curve for lower Pr_{in} values lies above those for higher Pr_{in} values demonstrating the presence of entrance effects. However, further downstream the Nu_m curve for $Pr_{in} = 1250$ lies above those for $Pr_{in} = 200$ and 50. This is because, even though ΔT was fixed at 30 K for the three Prandtl numbers, the variable viscosity effect is most pronounced for the $Pr_{in} = 1250$ case due to the steep slope of the v–T curve of the simulated fluid at lower temperatures (or higher Prandtl numbers). For instance, the maximum value of v^+ for $Pr_{in} = 1250$ is 6.05 as compared to 2.49 and 1.18 for $Pr_{in} = 200$ and 50, respectively. A higher value of v^+ for heating causes a larger viscosity gradient which offers lower resistance to the buoyancy-induced secondary flow, thereby enhancing the heat transfer. For the apparent friction factor, the curve for higher values of Pr_{in} generally lies below those for lower Pr_{in}. However, for $10^{-3} \leqslant z^+ \leqslant 10^{-2}$, which corresponds to the region where free convection effects dominate (as reflected by the plateau on the Nu_m plot), the $f_{app}Re_{in}$ values for $Pr_{in} = 200$ overshoot those for $Pr_{in} = 50$ by around 10%. This is due to the increased viscosity gradient which increases the secondary flow and, hence, the pressure drop. This effect is not seen for $Pr_{in} = 1250$ case as the associated near-wall viscosity is large enough to damp out the secondary flow brought upon by the viscosity gradient in the fluid.

The effect of ΔT for heating and cooling on Nu_m

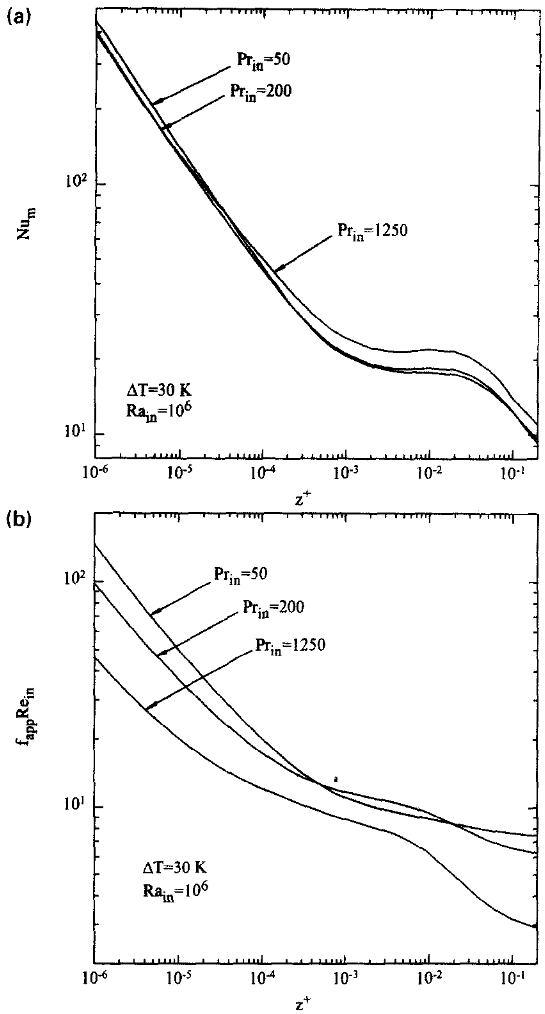

Fig. 3. (a) Effect of inlet Prandtl number on average Nusselt numbers for simultaneously developing mixed convection flow and heat transfer. (b) Effect of inlet Prandtl number on apparent friction factors for simultaneously developing mixed convection flow and heat transfer.

and $f_{app}Re_{in}$ for $Pr_{in} = 50$ and $Ra_{in} = 10^6$ is shown in Fig. 4(a) and (b), respectively. The Nusselt number increases with increasing ΔT for heating and decreases with increasing ΔT for cooling, as expected, for the entire range of z^+. When a liquid is heated, the liquid in the near-wall region is less viscous than that in the center. Consequently, the fluid velocity in the near-wall region is larger for a heated liquid than that for a unheated liquid at the same average temperature. Furthermore, the secondary flow is also increased due to lesser viscous resistance. Both these effects contribute to the increase in heat transfer during heating. The opposite is true for cooling, where the heat transfer is reduced. The maximum increase or decrease in Nu_m for heating or cooling as compared to the constant viscosity situation is around 15–20% for the range of parameters studied.

However, the effect of variable viscosity on the pressure drop is much more pronounced, as seen in Fig. 4(b). For instance, $f_{app}Re_{in}$ for heating with $\Delta T = 30$ K

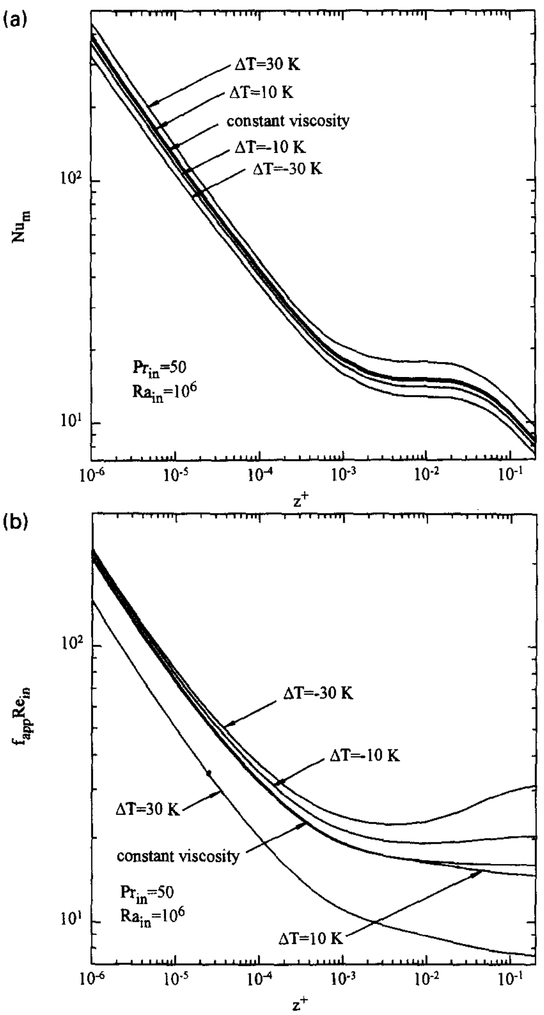

Fig. 4. (a) Effect of wall-to-inlet temperature difference on average Nusselt numbers for simultaneously developing mixed convection flow and heat transfer. (b) Effect of wall-to-inlet temperature difference on apparent friction factors for simultaneously developing mixed convection flow and heat transfer.

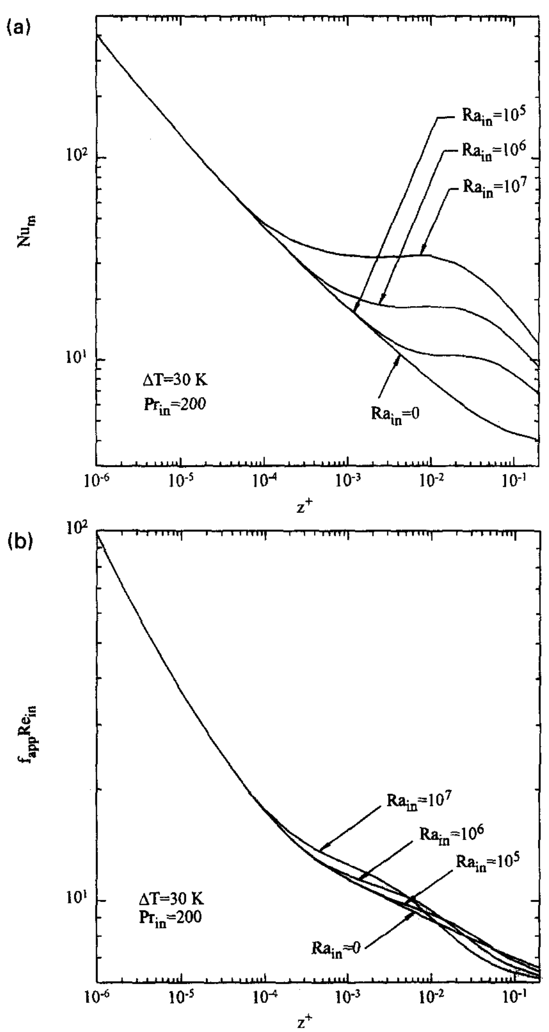

Fig. 5. (a) Effect of inlet Rayleigh number on average Nusselt numbers for simultaneously developing mixed convection flow and heat transfer. (b) Effect of inlet Rayleigh number on apparent friction factors for simultaneously developing mixed convection flow and heat transfer.

is lower than that for the constant viscosity case by around 50%. This reduction is primarily due to the reduction of liquid viscosity in the near-wall region due to heating. The increased secondary flow brought upon by heating is seen to be dominated by the effect of lower viscosity for the heating ranges considered in this study. For cooling, $f_{app}Re_{in}$ initially decreases with increasing z^+, indicating dominance of entrance effects, then attains a minimum, illustrating the balance between entrance and cooling effects, and then finally starts increasing with increasing z^+ as the cooling effect starts dominating. The location of the $f_{app}Re_{in}$ minima in the z^+ scale roughly corresponds to the location where constant viscosity, hydrodynamically fully developed flow is attained. The increase in $f_{app}Re_{in}$ is larger for flows with larger ΔTs (degree of cooling), as expected. These results indicate that constant viscosity assumption could lead to significant errors in predicting heat transfer and pressure drop for mixed convection flows. Especially, the error in pressure drop predictions could be significant even for small or moderate ΔTs.

The effect of inlet Rayleigh number, Ra_{in}, on the heat transfer and pressure drop for $Pr_{in} = 200$ and $\Delta T = 30$K is shown in Fig. 5(a) and (b), respectively. In the near-inlet region ($z^+ \leqslant 10^{-4}$), entrance effects dominate, which make the curves for different values of Ra_{in} almost indistinguishable from each other. Further downstream, the Nu_m profiles starts deviating from the forced convection ($Ra_{in} = 0$) profile, indicating the appearance of buoyancy effects. Further downstream, the profiles exhibit a plateau ($Nu_m \approx$ constant), indicating a balance between entrance and buoyancy effects, and then the curve drops sharply with increasing z^+ as the wall-to-bulk temperature difference diminishes. Finally, the Nu_m profiles for large z^+ appears to asymptotically approach the fully developed value of 3.66. However, since computations were carried out up to $z^+ = 0.2$ for computational economy, the asymptotic fully developed Nusselt number was not obtained in the present study. Qualitatively, the Nu_m profiles are similar to those presented in ref. [19].

The z^+ location where the Nu_m curve for mixed convection begins to depart from its forced convection counterpart can be estimated from the scaling analysis presented earlier. As discussed earlier, the departure occurs approximately when $\Delta = 1$. Thus, the z^+ location where transition from forced to free convection occurs is given by

$$z^+_{TR} \sim (Ra\mathscr{F})^{-1/2}. \qquad (20)$$

The effect of Ra_{in} on the apparent friction factor is somewhat more complicated. As seen in Fig. 5(b), at small values of $z^+ (z^+ \leqslant 10^{-4})$, the profiles are indistinguishable from each other as entrance effects dominate. For $10^{-4} < z^+ \leqslant 10^{-2}$, the $f_{app}Re_{in}$ curve for larger values of Ra_{in} lies above those for smaller Ra_{in} as the larger secondary flow associated with high values of Ra_{in} increases the pressure drop. For $z^+ > 10^{-2}$, the friction factor profiles cross over, and the $f_{app}Re_{in}$ curve for larger Ra_{in} lies below those for smaller Ra_{in}. This is because for larger values of Ra_{in}, the temperature profile develops faster due to increased mixing caused by secondary flow. The faster rate of thermal development, in turn, reduces the secondary flow as the wall-to-bulk temperature difference is diminished, leading to a decrease in the pressure drop.

The effect of the inlet velocity profile on Nu_m and $f_{app}Re_{in}$ is shown in Fig. 6(a) and (b), respectively. The thermally developing flow corresponds to a parabolic axial velocity profile at the inlet, while the simultaneously developing flow corresponds to a uniform axial velocity profile at the inlet. It may be noted that the former is realized in practice when a sufficiently long unheated flow length is provided prior to heating or cooling or for very high Prandtl number flow, while the latter is realized in the absence of any such unheated flow development length and, thus, is more realistic. The results indicate that the effect of the inlet velocity profile is present only in the near-inlet region where entrance effects are present. For larger values of z^+, the Nu_m and $f_{app}Re_{in}$ curves for these two cases are almost indistinguishable from each other. This observation is encouraging since it suggests that the same correlation developed for thermally developing flow can be applied to simultaneously developing flow in that region.

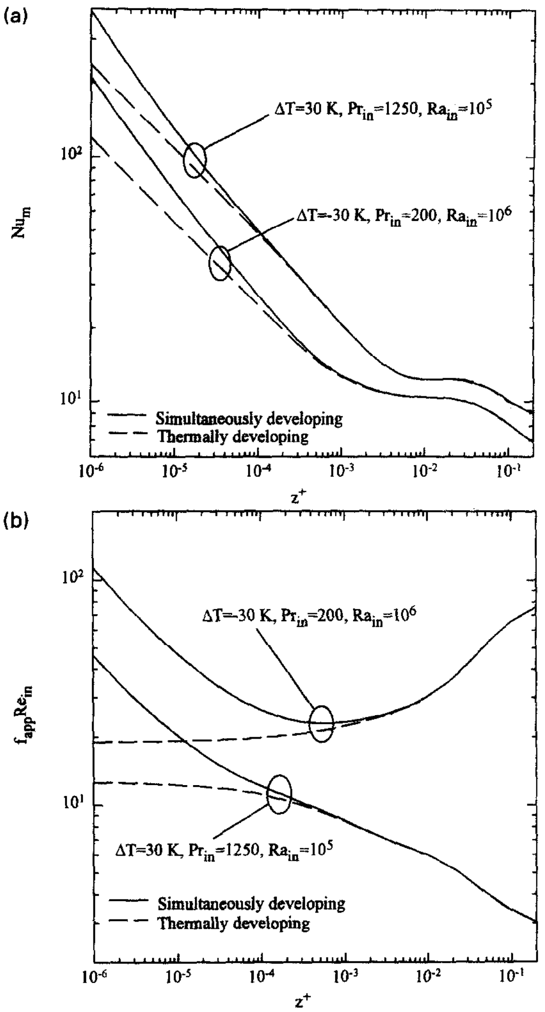

Fig. 6. (a) Effect of inlet velocity profile on average Nusselt numbers for simultaneously developing mixed convection flow and heat transfer. (b) Effect of inlet velocity profile on apparent friction factors for simultaneously developing mixed convection flow and heat transfer.

CORRELATIONS

The results obtained in the present study indicated that in the near-inlet region ($\Delta \leqslant 1$), where forced convection dominates, separate correlations are necessary for predicting Nusselt numbers for thermally developing and simultaneously developing flow and heat transfer. Thus, for ($\Delta \leqslant 1$), the average Nusselt number, Nu_m, was correlated as:

$$\frac{Nu_m}{Nu_{TD,CP}} = \begin{cases} (v^+)^{0.18} & \text{thermally developing} \\ (v^+)^{0.22}[1+0.067(z^+Pr)^{-0.62}]^{0.27} & \text{simultaneously developing} \end{cases} \qquad (21)$$

where $Nu_{TD,CP}$ is the length-averaged Nusselt number for constant property thermally developing forced convection flow, and is given [34] as:

$$Nu_{TD,CP} = \begin{cases} -0.5632+1.57z^{+^{-0.3351}}, & 10^{-6} \leqslant z^+ \leqslant 10^{-3} \\ 0.9828+1.129z^{+^{-0.3686}}, & 10^{-3} \leqslant z^+ \leqslant 10^{-2} \\ 3.6568+0.1272z^{+^{-0.7373}}\exp(-3.1563z^+), & z^+ > 10^{-2} \end{cases} . \qquad (22)$$

Table 4. Experimental database used for correlation in the present study

Reference	Data points	Re	Pr	$Ra/10^5$	μ_b/μ_w	L/D	Fluid
Kern and Othmer [5]	251	16–2420	39–2040	5.3–896 0	1.4–51.6	48 100 193	Oil
Oliver [8]	89	0.2–1580	5.5–15100	0.006–26.9	0.1–2.9	72	Ethyl alcohol, glycerol–water, water
Brown and Thomas [9]	85	235–1240	3.5–7.4	2.0–204	0.5–0.9	36 72 108	Water
Depew and August [11]	40	5–1810	5.7–391	2.0–141	0.3–0.8	28.4	Glycerol–water, water, ethyl–alcohol
Holden and White [36]	43	13–1380	137–714	2.7–10.1	2.4–12.4	119.2 113.3	Oil
Drew [37]	29	7–109	142–643	0.2–0.3	1.7–8.1	220	Glycerol–water
Marner and Bergles [38]	70	26–533	1150–7000	3.0–16.1	0.0048–42.8	100.43	Liquid polymer
Pentermann [39]	68	584–2000	230–268	9.4–15.9	0.1–4.7	143.88	Oil

However, for $\Delta > 1$, where natural convection effects dominate, a single equation is sufficient to correlate the Nusselt numbers for both thermally and simultaneously developing flow and heat transfer as:

$$Nu_m = 7.93Ra^{0.21}\mathscr{F}^{-0.05}\ln(1+0.13\Delta)/\Delta. \quad (23)$$

It may be noted that, in the near-inlet region, usage of v^+ rather than $\mathscr{F}$ correlates the heating and cooling data better, whereas for $\Delta > 1$, usage of $\mathscr{F}$ in the correlation works out better. Equation (23) is similar to the one proposed by Hieber [13], but uses a different parameter, Δ, instead of $Ra^{1/4}z^+$ as used by Hieber [13]. The proposed correlation predicts the experimental data obtained by eight different investigations (see Table 4) and the present numerical results within a r.m.s. error† of 10.6% and 16.6% for $\Delta \leqslant 1$ and $\Delta > 1$, respectively, and has an overall r.m.s error of 15.5% for the complete range of Δ. The correlation is valid in the range $0.0048 \leqslant \mu_w/\mu_b \leqslant 51.6$, $6\times10^2 \leqslant Ra \leqslant 10^8$, $2 \leqslant Pr \leqslant 15{,}100$, $10^{-6} \leqslant z^+ \leqslant 0.2$, and $Re \leqslant 2420$, which covers a wide spectrum of viscous liquids ranging from water to oils. The proposed correlation is an improvement over the existing ones both in terms of accuracy and wider range of applicability. The existing correlations were developed from smaller databases, and, hence, their accuracy degenerates when applied to the current large database comprising both numerical and experimental data for thermally developing flow, as shown in Table 5 (the correlations of Jackson *et al.* [7] and Yousef and Tarasuk [12] were not compared as they are valid for air only). For instance, the widely used correlation of Depew and August [11] was developed from their own data and a few selected datasets of Kern and Othmer [5], Oliver [8], and Brown and Thomas [9]. As a further check of the accuracy of the existing correlation, the Eubank and Proctor correlation [6] (see Table 5) was re-fitted using the current larger database. The re-fitted equation had a r.m.s. error of around 26% and is thus less accurate than the proposed one.

Similarly, the apparent friction factor for developing mixed convection flow and heat transfer was correlated as

for $\Delta \leqslant 1$:

thermally developing flow

$$\frac{f_{app}Re_{in}}{16} = 0.98\left(\frac{v_w}{v_{in}}\right)^{4.12}(v^+)^{3.98} \quad (24)$$

simultaneously developing flow

$$\frac{f_{app}}{f_{app,CP}} = \frac{v_w}{v_{in}}(v^+)^{0.88}[1+0.39(z^*)^{-0.29}]^{-0.45}. \quad (25)$$

For $\Delta > 1$:

thermally and simultaneously developing flow

heating

$$\frac{f_{app}}{16} = 3.19\frac{v_w}{v_{in}}Ra^{0.13}\mathscr{F}^{-2.31}\ln(1+0.07\Delta)/\Delta \quad (26)$$

cooling

$$\frac{f_{app}}{f_{app,CP}} = 1.36\frac{v_w}{v_{in}}(v^+)^{0.86}\Delta^{-0.07}(z^*)^{0.13} \quad (27)$$

where

$$\frac{f_{app,CP}Re}{16} = \frac{0.3016}{z^{*0.4634}} + \frac{1+0.1526/(10^3z^*)-0.4068z^{*-0.2192}}{1-1.693\times10^{-8}z^{*-0.5631}}. \quad (28)$$

Equations (24)–(27) predict the current friction fac-

† Error $= Nu_{correlation}/Nu_{data} - 1$

Table 5. Accuracy of available length-averaged Nusselt correlations for thermally developing flow when applied to current experimental and numerical database

Correlation	Minimum error(%)	Maximum error(%)	r.m.s. error(%)
Kern and Othmer [5]	−70.5	287.4	57.7
Eubank and Proctor [6]	−46.2	154.8	22.0
Oliver [8]	−63.4	320.3	38.6
Brown and Thomas [9]	−66.8	922.2	152.8
ESDU [10]	−25.5	402.5	52.6
Depew and August [11]	−64.4	153.3	39.1
Hieber [13]	−16.0	369.9	84.4
Palen and Taborek [14]	−57.1	790.1	117.4
Present correlation			
$\Delta \leqslant 1$	−30.7	86.5	10.6
$\Delta > 1$	−50.3	117.3	16.6
Overall			15.5

tor data of this study to within a r.m.s. error of 10.3, 7.0, 13.6, and 8.8%, respectively, and has the same range of validity as that of the Nusselt number correlation.

CONCLUSIONS

Numerical analysis of thermally developing and simultaneously developing mixed convection flow with variable viscosity for both heating and cooling were carried out. A scaling analysis was performed to find a parameter which was used to help correlate the available experimental and the present numerical data. From this study we can conclude that variable viscosity effects can be significant, being more pronounced on the friction factor than on the Nusselt numbers. Thus, variable viscosity effects should be included in the analysis in order to make accurate predictions. Buoyancy effects were found to be negligible in the near-inlet region where entrance effects dominate. Thus, the inlet velocity profile influences the heat transfer and pressure drop in the near-inlet region only.

The proposed correlations are more accurate and have a wider range of applicability than those now available in the literature. To the best of the authors' knowledge, correlations for predicting pressure drop in simultaneously developing mixed convection flow do not exist. Thus, these correlations should be of particular use to designers, provided they can be experimentally validated to some degree. Finally, this study has demonstrated that a judicious combination of scaling analysis, analysis of available experimental data, and accurate numerical modeling can be used as a useful tool for analysis and developing accurate thermal–hydraulic correlations.

Acknowledgments—This work was funded in part by the Rensselaer Polytechnic Institute High Temperature Technology Program, administered by the New York State Energy Research and Development Authority (NYSERDA) and by NYSERDA under agreement number 3097-EEED-IA-94. This support is greatly appreciated.

REFERENCES

1. A. E. Bergles, Experimental verification of analyses and correlation of the effects of temperature-dependent fluid properties on laminar heat transfers. In *Low Reynolds Number Flow Heat Exchangers* (Edited by S. Kakac, R. K. Shah and A. E. Bergles), pp. 473–486. Hemisphere, Washington, DC (1983).
2. W. Aung, Mixed convection in internal flow. In *Handbook of Single-Phase Convective Heat Transfer* (Edited by S. Kakac, R. K. Shah and W. Aung), pp. 15.1–15.51. Wiley, New York (1987).
3. S. Kakac, The effect of temperature-dependent fluid properties on convective heat transfer. In *Handbook of Single-Phase Heat Transfer* (Edited by S. Kakac, R. K. Shah and W. Aung), pp. 18.1–18.56. Wiley, New York (1987).
4. A. P. Colburn, A method for correlating forced convective heat transfer data and a comparison with fluid friction, *Trans. AIChE* **29**, 174–210 (1933).
5. D. Q. Kern and D. F. Othmer, Effect of free convection on viscous heat transfer in horizontal tubes, *Trans. AIChE* **39**, 517–555 (1943).
6. C. C. Eubank and W. S. Proctor, M. S. Thesis in Chemical Engineering, Massachusetts Institute of Technology, Cambridge, MA (1951).
7. T. W. Jackson, J. M. Spurlock and K. R. Purdy, Combined free and forced convection in a constant temperature horizontal tube, *AICHE J.* **7**, 38–41 (1961).
8. D. R. Oliver, The effect of natural convection on viscous-flow heat transfer in horizontal tubes, *Chem. Engng Sci.* **17**, 335–350 (1962).
9. A. R. Brown and M. A. Thomas, Combined free and forced convection heat transfer for laminar flow in horizontal tubes, *J. Mech. Engng Sci.* **7**, 440–448 (1965).
10. ESDU, Forced convection heat transfer in circular tubes, part II: data for laminar and transitional flow including free convection effects, Data Item No. 68006, London (1968).
11. C. A. Depew and S. E. August, Heat transfer due to combined free and forced convection in a horizontal isothermal tube, *J. Heat Transfer* **93**, 380–384 (1971).
12. W. W. Yousef and J. D. Tarasuk, Free convection effects on laminar forced convective heat transfer in a horizontal isothermal tube, *J. Heat Transfer* **104**, 145–152 (1982).
13. C. A. Hieber, Laminar mixed convection in an isothermal horizontal tube: correlation of heat transfer data, *Int. J. Heat Mass Transfer* **25**, 1737–1746 (1982).
14. J. W. Palen and J. Taborek, An improved heat transfer correlation for laminar flow of high Prandtl number

liquids in horizontal tubes, *AIChE Symp. Ser.* No. 245, **81,** 90–96 (1985).
15. E. N. Sieder and G. E. Tate, Heat transfer and pressure drop of liquids in tubes, *Indust. Engng Chem.* **28,** 1429–1435 (1936).
16. S. D. Joshi and A. E. Bergles, Analytical study of laminar flow heat transfer to pseudoplastic fluids in tubes with uniform wall temperature, *AIChE Symp. Ser.* **77,** 114–122 (1981).
17. C. A. Hieber and S. K. Sreenivasan, Mixed convection in an isothermal heated horizontal pipe, *Int. J. Heat Mass Transfer* **17,** 1337–1348 (1974).
18. L.-S. Yao, Free-forced convection in the entry region of a heated straight pipe, *J. Heat Transfer* **100,** 212–219 (1978).
19. J.-W. Ou and K. C. Cheng, Natural convection effects on Graetz problem in horizontal isothermal tubes, *Int. J. Heat Mass Transfer* **20,** 953–960 (1977).
20. M. Hishida, Y. Nagano, and M. S. Montesclaros, Combined forced and free convection in the entrance region of an isothermally heated horizontal pipe, *J. Heat Transfer* **104,** 153–159 (1982).
21. J. Pascal Courtier and R. Greif, An investigation of laminar mixed convection inside a horizontal tube with isothermal conditions, *Int. J. Heat Mass Transfer* **28,** 1293–1305 (1985).
22. D. Choudhury and S. V. Patankar, Combined forced and free laminar convection in the entrance region of an inclined isothermal tube, *J. Heat Transfer* **110,** 901–909 (1988).
23. C. Zhang and K. J. Bell, Mixed convection inside horizontal tubes with nominally uniform heat flux, *AIChE Symp. Ser.* **88,** 212–219 (1992).
24. G. J. Hwang and H. C. Lai, Laminar convective heat transfer in a horizontal isothermal tube for high Rayleigh number, *Int. J. Heat Mass Transfer* **37,** 1631–1640 (1994).
25. A. J. Ghajar and L. M. Tam, Correlations for forced and mixed convection in straight duct flows with three different inlet configuration. In *General Papers in Heat Transfer* (Edited by M. K. Jensen, R. Mahajan, E. McAssey, M. F. Modest, D. Pepper, M. Sohal and A. Lavine), HTD 204, pp. 49–56. ASME, New York (1992).
26. Y. Mori and K. Futagami, Forced convective heat transfer in uniformly heated horizontal tubes (2nd report, theoretical study), *Int. J. Heat Mass Transfer* **10,** 1801–1813 (1967).
27. S. M. Morcos and A. E. Bergles, Experimental investigation of combined forced and free convection in horizontal tubes, *J. Heat Transfer* **97,** 212–219 (1975).
28. D. A. Anderson, J. C. Tannehill, and R. H. Pletcher, *Computational Fluid Mechanics and Heat Transfer* (1st Edn), Chap. 5. Hemisphere, Washington, DC (1984).
29. A. Bejan, *Convective Heat Transfer* (1st Edn), Chaps 2–4. Wiley, New York (1984).
30. D. B. Spalding, Mathematical modeling of fluid mechanics, heat transfer, and chemical reaction processes—a lecture course, CFDU Report HTS/80/1 (1980).
31. R. K. Shah and A. L. London, Laminar forced convection in ducts. In *Adv. Heat Transfer* (Edited by T. F. Irvine and J. P. Hartnett), Suppl. 1. Academic, New York (1978).
32. K.-T. Yang, Laminar forced convection of liquids in tubes with variable viscosity, *J. Heat Transfer* **84,** 353–362 (1962).
33. D. E. Rosenberg and J. D. Hellums, Flow development and heat transfer in variable-viscosity fluids, *Indust. Engng Chem. Fund.* **4,** 417–422 (1965).
34. F. L. Test, Laminar flow heat transfer and fluid flow for liquids with temperature-dependent viscosity, *J. Heat Transfer* **90,** 385–393 (1968).
35. B. Shome and M. K. Jensen, Correlations for simultaneously developing laminar flow and heat transfer in a circular tube, *Int. J. Heat Mass Transfer* **36,** 2710–2713 (1993).
36. Holden and White, Thesis, Massachusetts Institute of Technology, Cambridge, M.A. (1927). (See T. B. Drew, J. J. Hogan, and W. H. McAdams, Heat transfer in stream-line flow, *Indust. Engng Chem.* **23,** 936–945 (1931).)
37. T. B. Drew, Heat Transfer in stream-line flow, II: Experiments with glycerol, *Indust. Engng Chem.* **2,** 152–157 (1932).
38. W. J. Marner and A. E. Bergles, Augmentation of highly viscous laminar heat transfer inside tubes with constant wall temperature, *Expl Therm. Fluid Sci.* **2,** 252–267 (1989).
39. A. W. Pentermann, The effects of temperature-dependent fluid properties on laminar heat transfer and pressure drop in internally finned tubes. M. S. Thesis, Rensselaer Polytechnic Institute, Troy, NY (1993).